Pergamon
www.elsevier.com/locate/asr
Available online at www.sciencedirect.com
SCIENCE DIRECT
doi: 10.1016/S0273-1177(03)00386-7

The GEOFLOW-EXPERIMENT ON ISS (Part II): NUMERICAL SIMULATION

Vadim Travnikov[1], Christoph Egbers, and Rainer Hollerbach

[1]*Department of Aerodynamics and Fluid Mechanics, BTU Cottbus, D-03046, Cottbus, Germany*

ABSTRACT

Convection in spherical shells under the influence of a radial force field is an important problem in classical convection theory. It is difficult to reproduce in a terrestrial laboratory though, because there gravity is everywhere downwards rather than radially inwards. It turns out that one can produce a radial force field, by applying a high voltage difference between the inner and outer spheres. The combination of the electric field and the temperature-dependence of the fluid's dielectric coefficient then produces an r^{-5} central force field. Of course, in a terrestrial laboratory one still has the external gravity as well. In order to eliminate this effect and produce a purely radial force field, an experiment is planned on the International Space Station. In this paper we will present the results of numerical simulations intended to assist in the design of this experiment, for example in choosing the optimal radius ratios. We solve for the onset of convection in such an r^{-5} force field, as a function of the radius ratio (varying between 0.3 and 0.6), the Prandtl number (varying between 1 and 100), and the Taylor number (measuring an overall rotation of the whole shell, which will also be possible in the experiment).

INTRODUCTION

We investigate convection induced by a radially symmetric electric field in a rotating spherical shell filled with dielectric fluid. The two concentric spherical shells are maintained at constant, different temperatures. The innere sphere is warmer and maintained at a constant temperature T_1 while the outer sphere is at a constant temperature T_2. The flow in this system then depends on the following parameters: the radius ratio $\eta = \frac{R_1}{R_2}$, the Prandtl number $Pr = \nu/k$, and the Taylor number $Ta = (2\Omega R_2^2/\nu)^2$. Additionally, the externally imposed electric field drives the actual convection. How the Rayleigh number depends on the strength of this field is derived in the next section. We will also consider both non-rotating ($Ta = 0$) as well as rotating ($Ta > 0$) convection.

The problem of convection in spherical shells has been considered before by many authors. Joseph and Carmi (1966) calculated the critical Rayleigh numbers via linear and energy stability analysis in the non-rotating case, for different central force fields. Roberts (1968) calculated the flow and the critical Rayleigh numbers in the limit of very rapid rotation, and found that the critical Rayleigh number depends on the Taylor number according to $Ra \sim Ta^{2/3}$. Our numerical results here are also in good agreement with this asymptotic limit. Busse (1970) also considered this case, and predicted that the flow should take the form of "columnar cells". Finally, Hart et al. (1986) also considered a problem similar to the one we consider here. They only considered a hemispherical shell though, rather than a full shell, as we do here. Also, they did not include the centrifugal force, so their results are only valid for small Ta.

This research is a numerical basis for the experiment on the ISS (International Space Station), that is being prepared in the Department of Aerodynamics and Fluid Mechanics of the Brandenburg University of Technology (Germany).

Adv. Space Res. Vol. 32, No. 2, pp. 181–189, 2003

Printed in Great Britain
0273-1177/$30.00 + 0.00

GOVERNING EQUATIONS

Electrodynamics And Convection Without Rotation (Ta = 0)

In their simplest, Boussinesq form the Navier-Stokes, energy and continuity equations, describing the convection problem are:

$$\rho_0\left[\frac{\partial \mathbf{U}}{\partial t} + (\mathbf{U}\cdot\nabla)\mathbf{U}\right] = -\nabla \mathrm{P} + \rho_0\nu\Delta\mathbf{U} + \mathbf{F} \tag{1}$$

$$\frac{\partial \mathrm{T}}{\partial t} + \mathbf{U}\cdot\nabla\mathrm{T} = \kappa\Delta\mathrm{T} \tag{2}$$

$$\nabla\cdot\mathbf{U} = 0 \tag{3}$$

with boundary conditions

$$\mathrm{T}(\mathrm{R}_1) = \mathrm{T}_1, \qquad \mathrm{T}(\mathrm{R}_2) = \mathrm{T}_2, \qquad \mathbf{U}(\mathrm{R}_1) = 0, \qquad \mathbf{U}(\mathrm{R}_2) = 0 \tag{4}$$

The force $\mathbf{F}$ is due to the effect of this external electric field on the dielectric fluid. It has the form:

$$\mathbf{F} = -\frac{1}{2}\mathbf{E}^2\nabla\epsilon \tag{5}$$

and must be considered together with Maxwell's equations

$$\mathrm{div}(\epsilon\mathbf{E}) = 0, \qquad \mathrm{rot}\mathbf{E} = 0 \tag{6}$$

Since variations in ϵ (and also in the density ρ) are small, we can make the usual linearization

$$\epsilon = \epsilon_0(1 - \gamma(\mathrm{T} - \mathrm{T}_2)) \tag{7}$$

$$\rho = \rho_0(1 - \alpha(\mathrm{T} - \mathrm{T}_2)) \tag{8}$$

Using (7), together with standard vector identities, we can then rewrite $\mathbf{F}$ as:

$$\mathbf{F} = -\frac{1}{2}\nabla(\epsilon\mathbf{E}^2 - \epsilon_0\mathbf{E}^2) + \frac{1}{2}\epsilon_0\gamma\mathrm{T}_2\nabla\mathbf{E}^2 - \frac{1}{2}\epsilon_0\gamma\mathrm{T}\nabla\mathbf{E}^2, \tag{9}$$

The first two terms can then be combined with the pressure. That is, it is only the third term that will actually drive any convection.

To discover then what $\nabla\mathbf{E}^2$ is, we return to (6), and make the equivalent of the Boussinesq approximation. That is, we have already incorporated the temperature dependence of ϵ in this buoyancy force we just derived (the factor γ). Everywhere else though we will treat ϵ as constant, in which case (6) easily yield

$$\mathbf{E} = \frac{1}{r^2}\frac{\mathrm{R}_1\mathrm{R}_2}{\mathrm{R}_2 - \mathrm{R}_1}V_0 sin(\omega t)\mathbf{e}_\mathrm{r} \tag{10}$$

where $V_o sin(\omega t)$ is the externally imposed, alternating voltage.

Averaging over this (very high frequency) alternating cycle therefore,

$$\nabla\mathbf{E}^2 = -\frac{4}{r^5}\left(\frac{\mathrm{R}_1\mathrm{R}_2}{\mathrm{R}_2 - \mathrm{R}_1}\right)^2 V_{rms}^2\mathbf{e}_\mathrm{r} \tag{11}$$

To nondimensionalize the equations (1) - (3) the following scales are used:

$$\begin{gathered}\text{Length } r = \mathrm{R}_2 r^*,\\ \text{Temperature } \mathrm{T} - \mathrm{T}_2 = \Delta\mathrm{T}\mathrm{T}^*,\\ \text{Velocity } U = \tfrac{k}{\mathrm{R}_2}U^*,\\ \text{Time scale } t = \tfrac{\mathrm{R}_2^2}{\kappa}t^*,\end{gathered}$$

Then, dropping *, the equations (1) - (3) in their nondimensionalized form become:

$$\mathrm{Pr}^{-1}\left[\frac{\partial \mathbf{U}}{\partial t} + (\mathbf{U}\cdot\nabla)\mathbf{U}\right] = -\nabla \mathrm{P}_{eff.} + \Delta\mathbf{U} + \frac{\mathrm{Ra}}{\beta^2}\frac{\mathrm{T}}{r^5}\mathbf{e_r} \tag{12}$$

$$\frac{\partial \mathrm{T}}{\partial t} + \mathbf{U}\cdot\nabla\mathrm{T} = \Delta\mathrm{T} \tag{13}$$

$$\nabla\cdot\mathbf{U} = 0 \tag{14}$$

Here $\mathrm{P}_{eff.} = \mathrm{P} + \frac{1}{2}\mathbf{E}^2\epsilon - \frac{1}{2}\epsilon_0\mathbf{E}^2$.

The boundary conditions are:

$$\mathbf{U}(\eta) = \mathbf{U}(1) = 0, \qquad \mathrm{T}(\eta) = 1, \qquad \mathrm{T}(1) = 0 \tag{15}$$

For the parameters defining the flow, we have the following expressions:

$$\text{Prandtl number } \mathrm{Pr} = \frac{\nu}{\kappa},$$
$$\text{Rayleigh number } \mathrm{Ra} = \frac{2\epsilon_0\gamma}{\rho_0\nu\kappa}V_{rms}^2\Delta\mathrm{T},$$
$$\text{Radius ratio } \beta = \frac{\mathrm{R_2}-\mathrm{R_1}}{\mathrm{R_1}}$$

Basic State Ta = 0

As in the case of classical Rayleigh-Bénard convection between two planes we have no motion here

$$\mathbf{U} = 0, \tag{16}$$

but simply a radially symmetric temperature distribution:

$$\mathrm{T}(r) = -\frac{\eta}{1-\eta} + \frac{\eta}{1-\eta}\frac{1}{r} \tag{17}$$

Convection With Rotation (Ta > 0)

Convection with rotation is a more complicated problem than without rotation. First, because of the Coriolis force, the problem no longer decouples into different spherical harmonics l. Instead, all l's must be considered together. (The m's still decouple though.) Second, if one includes the centrifugal force as well, the basic state is no longer $\mathbf{U} = 0$. Instead, the centrifugal will itself drive a nonzero (but still axisymmetric) flow, and the critical Rayleigh numbers one then computes will be for the onset of nonaxisymmetric instabilities of that more complicated basic state. For small rotation rates the influence of the centrifugal force is of course also small. But for Ta > 40000 and small Prandtl numbers it is very important. Furthermore, the bigger the Prandtl number, the more important the centrifugal force becomes.

The governing equations in this case are:

$$\rho_0\left[\frac{\partial \mathbf{U}}{\partial t} + (\mathbf{U}\cdot\nabla)\mathbf{U}\right] = -\nabla\mathrm{P} + \rho_0\nu\Delta\mathbf{U} + \mathbf{F} - 2\rho_0\boldsymbol{\Omega}\times\mathbf{U} + \rho\Omega^2\mathbf{s} \tag{18}$$

$$\frac{\partial \mathrm{T}}{\partial t} + \mathbf{U}\cdot\nabla\mathrm{T} = \kappa\Delta\mathrm{T} \tag{19}$$

$$\nabla\cdot\mathbf{U} = 0 \tag{20}$$

where $\mathbf{s}$ is the cylindrically radial vector.

To nondimensionalize the equations (1) - (3) we use the same scales as before.

$$\begin{aligned}\mathrm{Pr}^{-1}\left[\frac{\partial \mathbf{U}}{\partial t} + (\mathbf{U}\cdot\nabla)\mathbf{U}\right] = &- \nabla P_{eff.} + \Delta\mathbf{U} + \frac{\mathrm{Ra}}{\beta^2}\frac{\mathrm{T}}{r^5}\mathbf{e_r} \\ &- \sqrt{\mathrm{Ta}}\mathbf{e_z}\times\mathbf{U} - \mathrm{Ra}'\mathrm{Ts}\end{aligned} \tag{21}$$

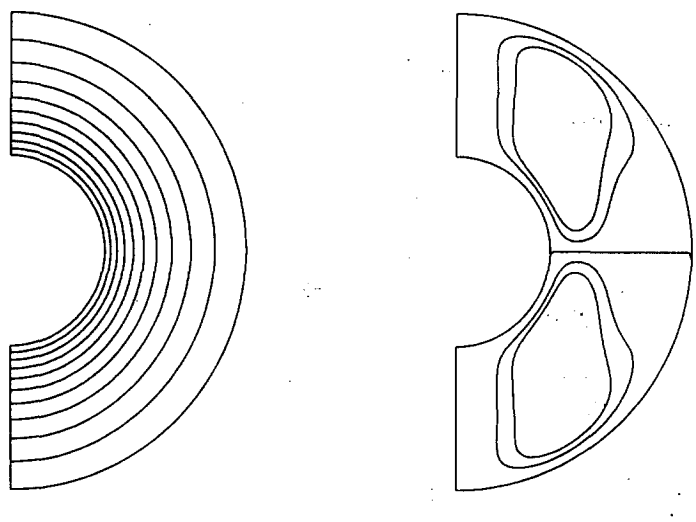

Fig. 1. The basic state for Ta> 0: left - Temperaturefield , right - streamfunction (equatorsymmetrical)

$$\frac{\partial \mathrm{T}}{\partial t} + \mathbf{U} \cdot \nabla \mathrm{T} = \Delta \mathrm{T} \tag{22}$$

$$\nabla \cdot \mathbf{U} = 0, \tag{23}$$

where the Taylor number $\mathrm{Ta} = (2\Omega \mathrm{R}_2^2/\nu)^2$ and $\mathrm{Ra}' = (\alpha \Delta \mathrm{T}/4)\mathrm{TaPr}$

Basic State Ta > 0

If we neglect the centrifugal force, we obtain the same basic state as in the non-rotating case. If we include the centrifugal force though, we also have a basic flow, and one which can only be computed numerically.

The equations (21) - (23) with boundary conditions (15) are to be solved numerically. This is done using the spectral code described by Hollerbach (2000). One example of the calculated basic flow can be seen in Figure 1. On the left is the temperature distribution, which we note is radially symmetric even for quite large Taylor numbers. On the right is the streamfunction of the meridional circulation.

LINEAR STABILITY ANALYSIS

We next wish to investigate the linear stability of these analytically (for $\mathrm{Ta} = 0$) or numerically (for $\mathrm{Ta} > 0$) determined basic states. We therefore begin by introducing

$$\mathbf{U}' = \mathbf{U} + \mathbf{u} \tag{24}$$

$$\mathrm{T}' = \mathrm{T} + \Theta \tag{25}$$

$$\mathrm{P}' = \mathrm{P}_{eff.} + p \tag{26}$$

where $\mathbf{U}$, T and $P_{eff.}$ are the basic state, and $\mathbf{u}$, Θ and p the perturbation quantities. We then substitute these expressions into the original equations, and neglect terms quadratic in the perturbation quantities.

Stability Analysis In Non-Rotating Case

Equations

The perturbation equations we obtain in the non-rotating case are

$$\mathrm{Pr}^{-1}\frac{\partial \mathbf{u}}{\partial t} = -\nabla p + \Delta \mathbf{u} + \frac{\mathrm{Ra}\,\Theta}{\beta^2 r^5}\mathbf{e_r} \tag{27}$$

$$\frac{\partial \Theta}{\partial t} + \mathbf{u}\cdot\nabla \mathrm{T} = \Delta\Theta \tag{28}$$

$$\nabla\cdot\mathbf{u} = 0 \tag{29}$$

The boundary conditions for the perturbations are of course no longer inhomogeneous; instead, they are simply

$$\mathbf{u}(\eta) = \mathbf{u}(1) = 0, \qquad \Theta(\eta) = \Theta(1) = 0 \tag{30}$$

From these equations we can immediately deduce one interesting result, namely that if the bifurcation is steady rather than oscillatory, so that at onset $\partial/\partial t = 0$, then the critical Rayleigh number will be independent of the Prandtl number. Of course, only the actual numerical results can reveal whether the onset is indeed steady rather than oscillatory. This turned out to be the case though.

Results

Calculations were carried out for different radius ratios $\eta = 0.1 - 0.9$ with a step $\Delta\eta = 0.02$ and $\mathrm{Pr} = 1, 10, 100$. The numerical simulations show the following results:

1. As already noted above, the initial onset of instability turned out to be steady in all cases. Ra_c therefore does not depend on Pr, but only on η and the spherical harmonic degree l. Figure 2 shows these Ra_c versus η curves, for $l = 1$ to 20.

2. We see then in Figure 2 that for narrower gaps (that is, as η tends to 1) Ra_c increases, and the most unstable mode shifts to higher and higher l.

3. We also see that for $\eta > 0.6$ or so it becomes increasingly difficult to distinguish the most unstable mode, because different modes are so close, and transitions from one mode to the next occur so quickly. This is therefore a parameter regime that we will want to avoid in designing the experiment. Since there are also technical difficulties in making the inner sphere too small, the specific radius ratios we will concentrate on in future work will be $\eta = 0.3$, 0.4 and 0.5, where the most unstable modes are $l = 2$, 3 and 4, respectively. This determination of the optimal radius ratios is the most important result to emerge from these preliminary calculations.

4. Finally, we just note that timesteps of 0.001 were sufficiently small to ensure convergence in all cases.

Stability Analysis In Rotating Case

Equations

The perturbation equations are now

$$\begin{aligned}\mathrm{Pr}^{-1}\left[\frac{\partial \mathbf{u}}{\partial t} + (\mathbf{U}\cdot\nabla)\mathbf{u} + (\mathbf{u}\cdot\nabla)\mathbf{U}\right] = &- \nabla p + \Delta\mathbf{u} + \frac{\mathrm{Ra}\,\Theta}{\beta^2 r^5}\mathbf{e_r} \\ &- \sqrt{\mathrm{Ta}}\mathbf{e_z}\times\mathbf{u} - \mathrm{Ra}'\Theta\mathbf{s}\end{aligned} \tag{31}$$

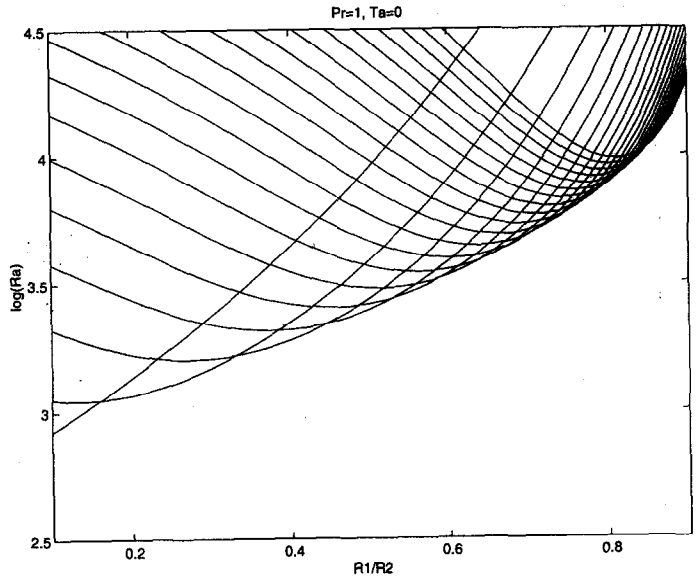

Fig. 2. Stability curve: critical Rayleigh number as function of η, for $l = 1$ to 20, increasing from left to right.

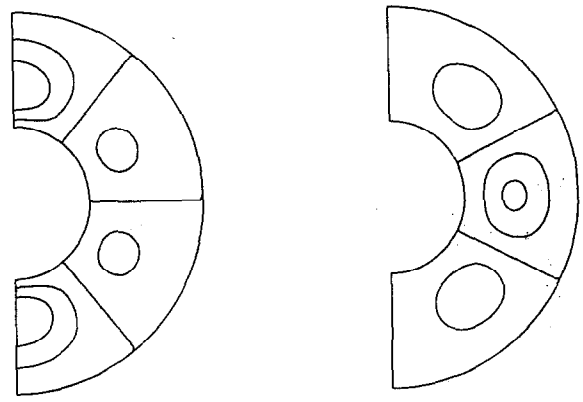

Fig. 3. An example of the perturbation solution, with the temperature on the left, and the meridional circulation on the right.. This particular solution corresponds to $\mathrm{Pr} = 1$, $\eta = 0.4$, $\ell = 3$

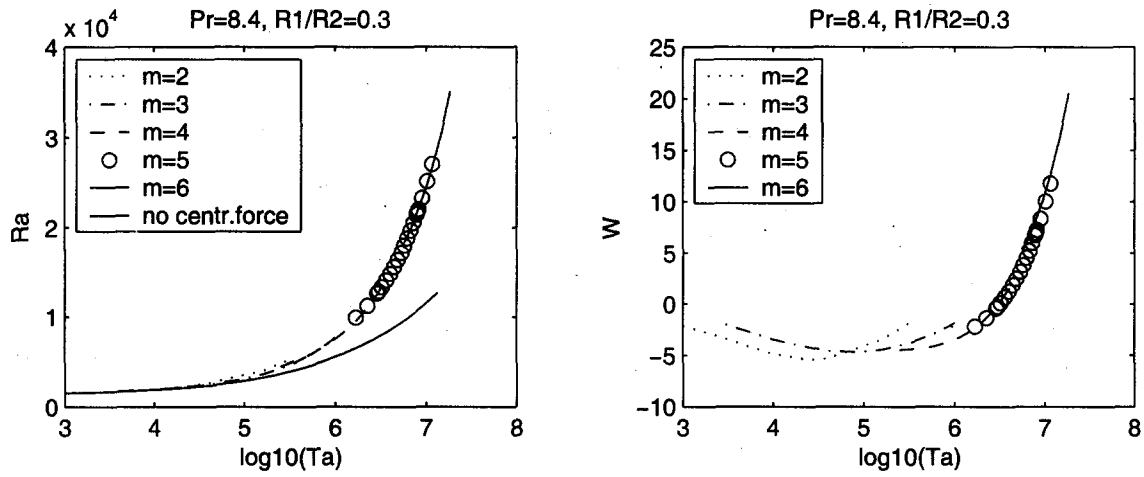

Fig. 4. a - Stability curve: critical Rayleigh number as function of Ta; b - Drift velocity as function of Ta

$$\frac{\partial \Theta}{\partial t} + \mathbf{U} \cdot \nabla \Theta + \mathbf{u} \cdot \nabla \mathrm{T} = \Delta \Theta \tag{32}$$

$$\nabla \cdot \mathbf{u} = 0, \tag{33}$$

with the same homogeneous boundary conditions as before. We have investigated the stability of the basic flow for fluids with Prandtl numbers Pr = 8.4, Pr = 38.96 and Pr = 101.38. The stability curves (a) are represented in figures below for these cases. The curves (b) represent the azimuthal drift velocity of the perturbations.

Results

We have investigated the stability of the basic flow for fluids with Prandtl numbers Pr = 8.4, Pr = 38.96 and Pr = 101.38. The results of this research are summarised in the Figure 4, Figure 5 and Figure 6. On the Figure 4 and Figure 5 the difference between critical Rayleigh numbers with and without of influence of the centrifugal force can be seen. The curve below corresponds to the case, if the centrifugal force is neglected. As we can see, the centrifugal force is very important even for small Taylor numbers.

From these results we can draw the following conclusions:

1. For fixed Prandtl and Taylor numbers the critical Rayleigh number is larger for narrower gaps, just as it was in the non-rotating case.
2. Even though these solutions now do depend on the Prandtl number (because this drift in longitude now means that $\partial/\partial t \neq 0$), they have very similar characteristics for all Pr.
3. For very large Ta the results do indeed tend to the $\mathrm{Ra} \sim \mathrm{Ta}^{2/3}$ asymptotic scaling deduced by Roberts.
4. The computational requirements are considerably greater than before, first of all because (as noted above) this is now a two- rather than one-dimensional problem, with all the different l's coupled together for a given m (truncations on the order of $l = 30$ were sufficient). Secondly, the timestep now had to be considerably smaller, with timesteps as small as 10^{-6} required at the largest Taylor numbers.

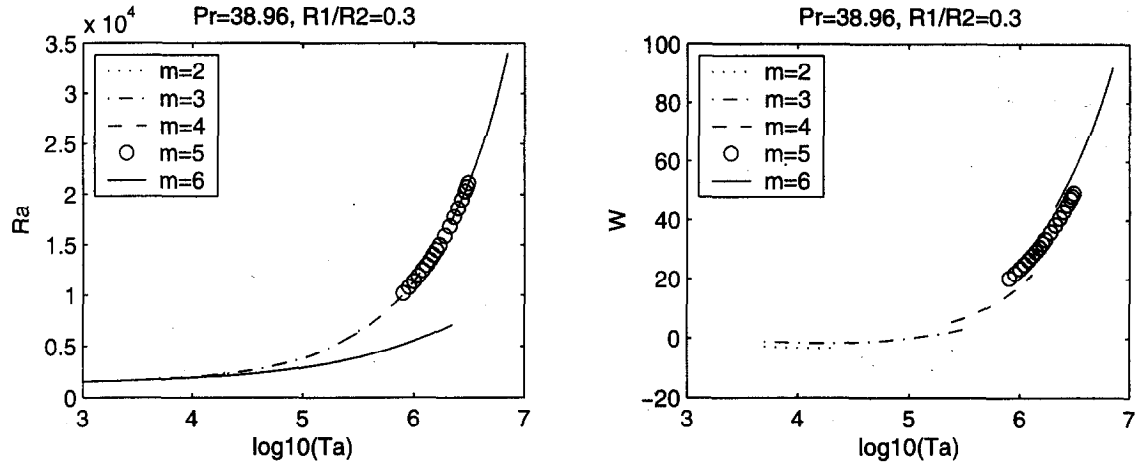

Fig. 5. a - Stability curve: critical Rayleigh number as function of Ta; b - Drift velocity as function of Ta

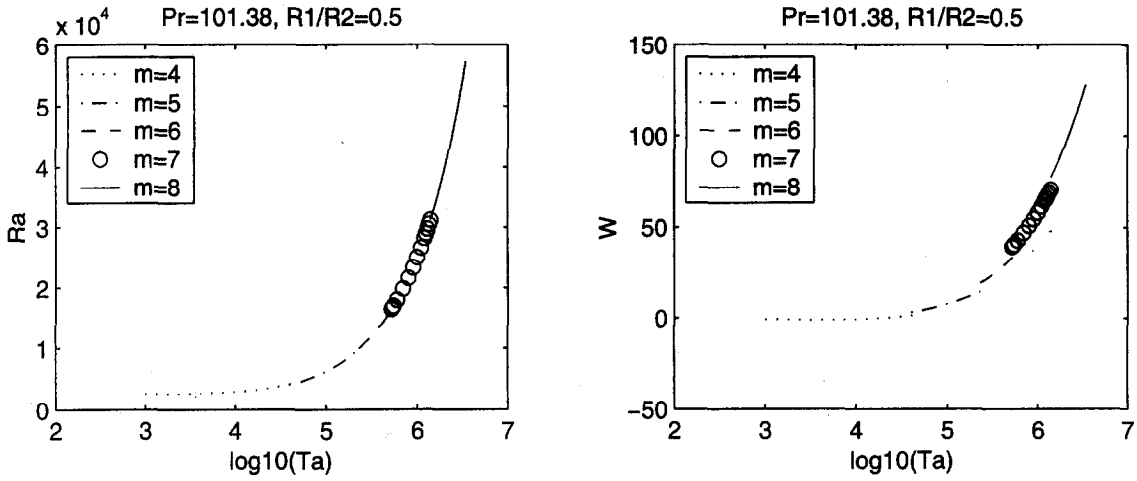

Fig. 6. a - Stability curve: critical Rayleigh number as function of Ta; b - Drift velocity as function of Ta

ACKNOWLEDGEMENTS

This work is supported by DLR - Deutsches Zentrum fuer Luft- und Raumfahrt e.V. under grant 50WM0122. RH's visit in Germany was supported by the Alexander von Humboldt Foundation.

REFERENCES

Busse, F. H., Thermal instabilities in rapidly rotating systems, *J. Fluid Mech.*, **44**(3), 441-460, 1970.

Carmi, S., and D. D. Joseph, Subcritical convective instability. Part 2. Spherical shells, *J. Fluid Mech.*, **26**, 769-778, 1966.

Hart, J. E., G. A. Glatzmaier, and J. Toomre, Space-laboratory and numerical simulations of thermal convection in a rotating hemispherical shell with radial gravity, *J. Fluid Mech.*, **173**, 519-544, 1986.

Hollerbach, R., A spectral solution of the magneto-convection equations in spherical geometry, *Int. J. Numer. Meth. Fluids*, **32**, 773-797, 2000

Roberts, P.H., On the thermal instability of a rotating-fluid sphere containing heat sources, *Phil. Trans. Roy. Soc. Lon. A*, **263**, 93-117, 1968.

E-mail address of V. Travnikov travnik@TU-Cottbus.De

Manuscript recieved 20 December 2002; revised 30 April 2003; accepted 5 February 2003